Hybrid Materials Hot Paper

International Edition: DOI: 10.1002/anie.201916002
German Edition: DOI: 10.1002/ange.201916002

Encapsulation of a Porous Organic Cage into the Pores of a Metal–Organic Framework for Enhanced CO_2 Separation

*Jun Liang, Alexander Nuhnen, Simon Millan, Hergen Breitzke, Vasily Gvilava, Gerd Buntkowsky, and Christoph Janiak**

Abstract: *We present a facile approach to encapsulate functional porous organic cages (POCs) into a robust MOF by an incipient-wetness impregnation method. Porous cucurbit-[6]uril (CB6) cages with high CO_2 affinity were successfully encapsulated into the nanospace of Cr-based MIL-101 while retaining the crystal framework, morphology, and high stability of MIL-101. The encapsulated CB6 amount is controllable. Importantly, as the CB6 molecule with intrinsic micropores is smaller than the inner mesopores of MIL-101, more affinity sites for CO_2 are created in the resulting CB6@MIL-101 composites, leading to enhanced CO_2 uptake capacity and CO_2/N_2, CO_2/CH_4 separation performance at low pressures. This POC@MOF encapsulation strategy provides a facile route to introduce functional POCs into stable MOFs for various potential applications.*

Introduction

There has been intense interest in the development of new porous materials for the selective capture and separation of important gases such as carbon dioxide.[1] In this regard, crystalline materials with extended porous structures such as zeolites,[2] coordination polymers (CPs) or metal–organic frameworks (MOFs),[3,4] and covalent organic frameworks (COFs)[5] are being widely investigated. The tunable pore sizes and high surface areas of these classes of materials make them suitable for trapping various guests. Porous organic molecules such as porous organic cages (POCs)[6] and porous macrocyclic molecules[7] have also been the subject of significant research during the past decade. Yet, it is usually difficult to prepare POC-based materials with high surface areas, and high degrees of gas sorption.[8] At the same time, the unique properties and easy availability of some POCs render them attractive in various fields including gas sorption and separation.[9] One such example is cucurbit[6]uril (CB6; see Scheme 1), which features a barrel-shaped rigid porous structure with only two windows and has been employed in various applications from gas capture to catalysis.[10] However, the application scope of the CB6 cage is limited by its poor solubility, strong intermolecular interactions, high affinity towards metal ions, and low surface area.[11] It is highly desirable to obtain POC-based hybrid materials with high porosity and stability by facile approaches, without sacrificing the inherent properties of the POCs.[12]

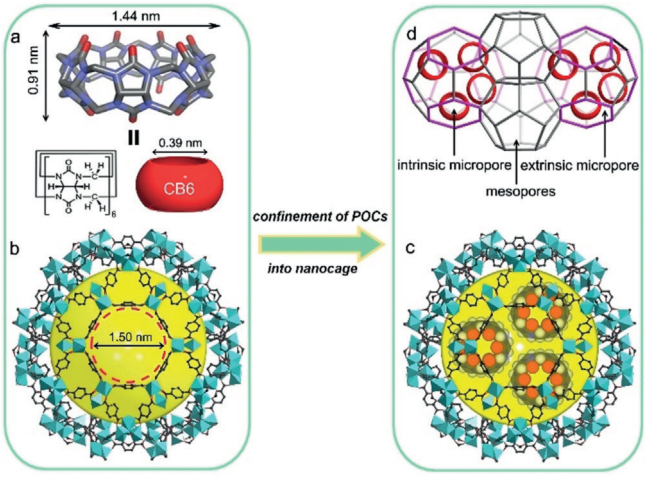

Scheme 1. The host-in-host concept for creating functional hybrid materials by the incorporation of CB6 into Cr-based MIL-101. Schematic views of a) the porous CB6 molecule; b) the mesoporous cage with hexagonal windows in MIL-101; c) CB6 in the larger cage of MIL-101; d) CB6 being selectively doped into the larger cages in MIL-101 while leaving the smaller cages empty. Hexagonal windows in pink. Hydrogen atoms are omitted for clarity.

Traditional strategies to obtain solid porous-organic-molecule-based porous materials can be briefly summarized: 1) Frameworks based on supramolecular bonds or coordination bonds (Figure 1 a);[8d,9a,c,d,13] 2) POCs covalently anchored in porous networks to provide active domains (Figure 1 b);[14] and 3) POCs dispersed as a porous additive in organic

[*] Dr. J. Liang, Prof. Dr. C. Janiak
Hoffmann Institute of Advanced Materials
Shenzhen Polytechnic
7098 Liuxian Blvd, Nanshan District, Shenzhen 518055 (China)
Dr. J. Liang, A. Nuhnen, S. Millan, V. Gvilava, Prof. Dr. C. Janiak
Institut für Anorganische Chemie und Strukturchemie
Heinrich-Heine-Universität Düsseldorf
40204 Düsseldorf (Germany)
E-mail: janiak@uni-duesseldorf.de
H. Breitzke, Dr. G. Buntkowsky
Eduard-Zintl-Institut für Anorganische und Physikalische Chemie
Technische Universität Darmstadt
Alarich-Weiss-Straße 4, 64287 Darmstadt (Germany)
Supporting information and the ORCID identification number(s) for the author(s) of this article can be found under: https://doi.org/10.1002/anie.201916002.

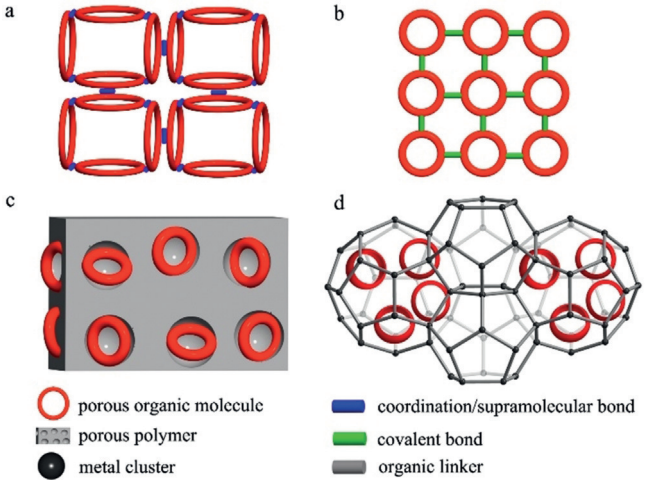

Figure 1. Strategies to generate porous materials containing porous organic molecules as a) neat frameworks, b) covalently anchored docking sites in a network, and c, d) functional guest molecules embedded in a polymer and a MOF, respectively.

polymers (Figure 1 c).[15] Although the assembly of POC units directed by metal ions or supramolecular interactions (Figure 1 a) is suitable for most POCs to give microporous frameworks, the disadvantages of these materials for practical applications are their low stability, macroscopic size, low surface areas, and polymorph issues.[16] While the covalent anchoring approach is highly programmable (Figure 1 b), it requires that the molecules can be readily modified for the required bond formation as elegantly demonstrated by Coskun, Kim, and others.[14] POCs/polymers can also be obtained by physical doping for gas sorption and separation as shown by Cooper and others.[15] Herein, we demonstrate for the first time that a POC can be confined in the pores of a host framework such as a MOF (Figure 1 d), and that the inherent properties of both POC and MOF can be combined in the resulting doubly porous hybrid material.

The highly ordered lattice and tunable pore sizes of MOFs have been used to accommodate polyoxometalates,[17] metal complexes,[18] metal–organic polyhedra,[19] metal nanoparticles,[20] and ionic liquids[21] as functional guests. These MOF-based host–guest composites have been obtained by various methods including incipient-wetness impregnation.[22] However, to the best of our knowledge, there is no report on fabricating functional porous hybrids by encapsulating a POC in the pores of a MOF. We demonstrate here that POC@MOF is a new "host-in-host" system with enhanced performance in CO_2 adsorption and CO_2/N_2, CO_2/CH_4 separation up to 1 bar, a proof of principle for the impetus to develop further POC@MOF materials.

Results and Discussion

As a proof of concept, we used CB6 as the model POC and MIL-101 as the host framework. CB6 has a rigid porous structure with hydrophobic cavities and an outer diameter of 1.44 nm and a height of 0.9 nm (Scheme 1 a),[11a] and a high affinity for molecules, such as dihalogens, CO_2, and acetylene through host–guest interactions or hydrogen bonding.[9e,11c,23] MIL-101, a robust MOF created by the Férey group, contains two kinds of mesopores with cage diameters of 2.9 nm and 3.4 nm.[18] The smaller cage has pentagonal windows with an aperture of approximately 1.2 nm, while the larger cage possesses both pentagonal and hexagonal windows with an opening of 1.5 nm (Scheme 1 b). As the molecular size (1.44 nm) of CB6 is smaller than the hexagonal window size (1.5 nm), and the inner surface of MIL-101 is more hydrophilic than the outer surface,[19] CB6 molecules could be readily encapsulated in the larger pores of MIL-101 by incipient-wetness impregnation (Scheme 1 c). The proper molecular size is, of course, important for the guest impregnation. Cucurbit[8]uril (CB8), with an outer diameter of 1.75 nm and a height of 0.9 nm, proved to be difficult to be encapsulated in MIL-101 by the wet impregnation method (see the Supporting Information for details).

Generally, CB6 was first fully dissolved in hydrochloric acid (37 wt %) solution before being added slowly to the degassed MOF at room temperature. After stirring for enough time to reach diffusion equilibrium, the obtained materials were washed successively with an excess amount of HCl (37 wt %) solution, deionized water, and ethanol (see the Supporting Information for details). Once CB6 has been encapsulated into the MOF pore, the leaching of CB6 could be hindered by the magnitude of the C–H···π and π···π interactions between CB6 and the terephthalic linkers of MIL-101.[11d] The obtained POC@MOF materials are denoted as CB6@MIL-101-W (W = 19, 29, or 36), where W represents the weight percentage of encapsulated CB6 in the material based on postsynthetic elemental analysis and ^{1}H NMR spectroscopy of digested samples.

The powder X-ray diffraction (PXRD) patterns of CB6@MIL-101 composites were similar to those of MIL-101 (Figure 2 a),[17] indicating the preserved crystalline framework

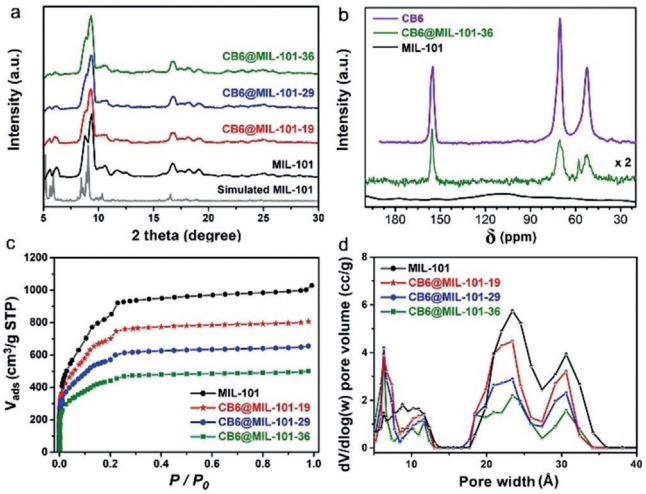

Figure 2. a) PXRD patterns and b) solid-state ^{13}C NMR spectra of the materials. c) N_2 adsorption isotherms at 77 K (see the Supporting Information for desorption isotherms) and d) pore size distributions of MIL-101 and CB6@MIL-101-W (W = 19, 29, 36) based on nonlocal density functional theory (NLDFT) calculations.

during the encapsulation process. Moreover, the intensity of the peaks at around 6° was gradually reduced with increasing CB6 loading, which was attributed to the filling of the MIL-101 pores with CB6. This phenomenon was also observed in previous publications, where the pores of MIL-101 were filled with drugs or polyamines.[24]

The successful encapsulation of CB6 in MIL-101 was supported by Fourier transform infrared (FT-IR) spectroscopy and NMR spectroscopy. The IR spectra of all composites display the characteristic vibration bands of both CB6 and MIL-101 (see the Supporting Information, Figure S2). The relative intensities of the IR bands of CB6 increased upon increasing the amount of CB6 in the composites. The ^{13}C solid-state NMR spectrum of CB6 shows three peaks (Figure 2b) at $\delta = 155.05$, 70.42, and 52.42 ppm, which were attributed to the C=O, CH, and CH_2 groups in CB6.[25] In contrast, solid MIL-101 shows no obvious NMR signals because of the paramagnetic Cr centers.[19] As expected, CB6@MIL-101-36 also shows the characteristic peaks of CB6. The intensities of the resonances are lower than those of neat CB6 because of the dilution of CB6 in the POC@MOF hybrid. Based on the solution ^1H NMR spectra of digested CB6@MIL-101 hybrids (Figures S3–S5), the molar ratio of terephthalic linker to CB6 was matched with the results based on elemental analysis for each sample (Table S1).

Scanning electron microscopy (SEM) analyses of CB6 and CB6@MIL-101 composites showed that the hybrids retained similar particle shapes and sizes (0.5–2 μm) as MIL-101, which are much smaller than that of CB6 crystallites (ca. 100 μm; Figure S6). To investigate if crystallites of CB6 had formed in a mixture with MIL-101 crystallites or if CB6 molecules had adsorbed only on the outer surface of MIL-101 in the composites, leaching experiments were conducted in $CsCl/D_2O$ solution (Figure S7).[26] The CB6@MIL-101 composites did not show any significant loss of CB6, while CB6 bulk crystals underwent ready dissolution. This further supports the effective encapsulation of CB6 into the pores of MIL-101.

To investigate the thermal stabilities of the composites, PXRD patterns were collected for each sample at elevated temperature in air. The results suggest that these composites are stable up to 300 °C, which is in accordance with the thermogravimetric analysis (TGA; Figures S8–S11).

The porosities of CB6, MIL-101, and all composites were investigated by recording nitrogen sorption isotherms at 77 K, showing the expected type Ib isotherms for the MIL-101 materials due to their wider micropores and narrow mesopores (Figures 2c, S12, and S13).[27] The Brunauer–Emmett–Teller (BET) surface areas of CB6, MIL-101, and CB6@MIL-101-W (W = 19, 29, 36) were found to be 185, 3219, 2655, 2117, and 1651 $m^2 g^{-1}$, respectively (Table S2). Compared with pure MIL-101, the surface areas and pore volumes of the composites gradually decreased because of the occupation of the mesopores of MIL-101 with increasing numbers of CB6 molecules (Table S2). Remarkably, CB6@MIL-101-36 still retained a BET surface area of 1651 $m^2 g^{-1}$ with a total pore volume of approximately 0.76 $cm^3 g^{-1}$ (at $P/P_0 = 0.9$), positioning CB6@MIL-101-36 among macrocycle-based materials with the highest porosity ever reported.[9a] The pore size distribution (PSD) of the composites changed with respect to MIL-101. Comparatively more distinct micropores (6 Å) appeared in these hierarchical hybrids and the mesopore volume was lost, which indicated the successful encapsulation of CB6 (Figure 2d). The intrinsic pores of CB6 and the newly formed extrinsic pores between CB6 and the pore walls of MIL-101 should facilitate selective gas sorption and separation processes (Scheme 1d).

To demonstrate that the host-in-host or POC@MOF approach can merge the merits of POCs and MOFs, we investigated the CO_2 and N_2 sorption of CB6, MIL-101, and CB6@MIL-101-W (W = 19, 29, 36) composites up to 1 bar at 293 K (Figure S14). As porous CB6 molecules with high affinity for CO_2 are encapsulated into the pores of MIL-101, these hybrids should show enhanced CO_2 capture and separation performance.[11c,22] Indeed, CB6@MIL-101-W (W = 19, 29, 36) exhibited much higher CO_2 uptake capacities of 68.5, 84.4, and 79.2 $cm^3 g^{-1}$, respectively, than MIL-101 and CB6 (44.3 and 36.7 $cm^3 g^{-1}$, respectively) at 1 bar (Figure 3a).

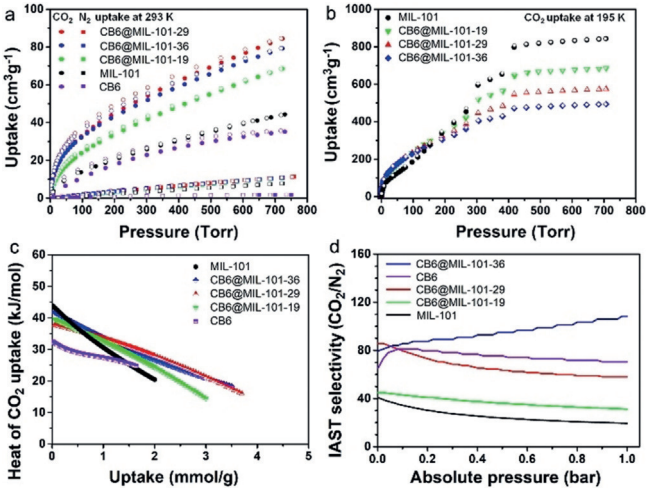

Figure 3. a) CO_2 and N_2 sorption isotherms of CB6, MIL-101, and composites measured up to 1 bar at 293 K. b) CO_2 sorption isotherms of MIL-101 and composites measured up to 1 bar at 195 K. c) Isosteric heats of adsorption (Q_{st}) of CO_2 for the materials. d) CO_2/N_2 selectivity of the materials measured by the IAST technique for a 15:85 (molar ratio) gas mixture of CO_2/N_2 at 293 K.

Notably, the CO_2 adsorption isotherm curves of all hybrids are steeper at low relative pressures than those of CB6 and MIL-101, indicating the higher affinity of these hybrids for CO_2. At the same time, the higher CO_2 uptake demonstrates the CO_2 accessibility of the intrinsic pores of CB6 and the mesopores and extrinsic micropores of CB6@MIL-101 (see Scheme 1d) at ambient conditions. Thereby, the CO_2 sorption studies rule out simple pore blocking by CB6 incorporation into the pore mouths only in MIL-101.

To further confirm this hypothesis, CO_2 adsorption isotherms of MIL-101 and the hybrids were obtained at 195 and 273 K (Figure 3b and Figure S15). The saturated CO_2 uptake capacities of these hybrids at 195 K and 1 bar are lower than that of MIL-101 because of their decreased pore volume (Figure 3b and Table S2). However, all composites

show significantly higher uptake at relatively low pressure up to 115 torr (Figure S16), which is the crucial pressure range for potential applications such as post-combustion CO_2 capture. The high affinity for CO_2 is further reflected by the isosteric heat of adsorption (Q_{st}). The Q_{st} values of CO_2 on CB6, MIL-101, and composites were estimated from the CO_2 adsorption data at 273 and 293 K (Figures 3c, S15, and S17–S21). The Q_{st}^0 values were calculated to be 33.2 and 43.9 kJ mol^{-1} for CB6 and MIL-101, respectively, due to the intrinsic pores of CB6 and the coordination of CO_2 onto the Lewis acidic chromium sites in activated MIL-101.[11c,28] The hybrid materials have relatively high Q_{st}^0 values (above 37 kJ mol^{-1}) because of the strong interactions between CO_2 and porous CB6 or Cr^{3+} sites in the composites. The lower Q_{st}^0 value of the CO_2 adsorption on CB6@MIL-101 in comparison to pure MIL-101 might be caused by the "sheltering effect", which makes some coordinative unsaturated sites (CUSs) unavailable to CO_2. Nevertheless, this is compensated for by CB6 offering more affinity sites and micropores for CO_2, which led to the enhanced uptake up to 1 bar at 293 K. The CO_2 uptake capacity of these composites is comparable or even higher than that of some amine/polyamine-modified MIL-101 materials (Table S4).[29] The strong sorption of CO_2 in CB6@MIL-101 was also confirmed in an FT-IR spectroscopic study. The IR spectrum of CB6@MIL-101-36 taken after exposure to CO_2 at 856 torr shows a CO_2 band at around 2338 cm^{-1} at room temperature, which indicates the interactions between CB6 and CO_2 (Figure S22).[11c] In contrast, the N_2 uptake of all hybrids only increased slightly when the amount of doped CB6 in MIL-101 was gradually increased (Figure 3a).

To simulate flue gas conditions, we calculated the CO_2/N_2 selectivities for CB6, MIL-101, and CB6@MIL-101-W (W = 19, 29, 36) from the N_2 and CO_2 adsorption isotherms using ideal adsorbed solution theory (IAST) for a CO_2/N_2 mixture (15:85) at 293 K (Figure 3d and Figure S23). For post-combustion CO_2 capture, porous sorbents should have both high CO_2 uptake capacities (in the low P/P_0 region) and high CO_2/N_2 selectivity. The IAST values for MIL-101, CB6, and CB6@MIL-101-W (W = 19, 29, 36) were determined to be 19, 70, 31, 58, and 108 at 293 K, respectively. The encapsulation of CB6 into MIL-101 allowed us to introduce CO_2 selectively because of the intrinsic micropores of CB6 and the retained micropores of MIL-101, while losing some of the uptake capacity of the non-selective mesopores of MIL-101. Thus, the combined properties of CB6 and MIL-101 showed a CO_2/N_2 selectivity increase from 31 to 108, upon loading CB6 into MIL-101. We believe that the hydrogen bonding and local dipole/quadrupole interactions between CB6 and CO_2 also play a role in the selectivity increase.[11c] Furthermore, a high concentration of CB6 in MIL-101 is critical to achieving high CO_2/N_2 selectivity. With an increase in the loading amount from 29 to 36 wt%, the selectivity increased to 58 and 108, respectively. A similar "cage effect" for enhancing CO_2 uptake and separation was also found in porous organic cage based nanoporous polymers by Coskun and co-workers.[14a]

Encouraged by the enhanced CO_2 uptake and CO_2/N_2 selectivity based on IAST predictions, we simulated breakthrough curves with a gas mixture of N_2/CO_2/He (42.5:7.5:50 v/v/v) at 293 K based on the DSLAI-fitted isotherm data of CB6, MIL-101, and composites, respectively (see the Supporting Information for details). The simulated breakthrough plot in Figure S24 shows an immediate rise in the N_2 concentrations at the outlet, indicating the comparably small N_2 sorption capacity of these porous materials under the chosen conditions. In contrast, CO_2 could be retained for about 3 min g^{-1} in CB6 and 4 min g^{-1} in MIL-101, which were close to the experimental breakthrough values (3.32 min g^{-1} and 3.35 min g^{-1}) reported separately for CB6 and MIL-101.[30] For CB6@MIL-101-36 the simulation gave an increased retention time of CO_2 of about 10 min g^{-1}, which is due to its higher uptake capacity and superior CO_2/N_2 selectivity with respect to the individual components under the given conditions. We note, however, that breakthrough experiments would still be part of a non-continuous separation process where the packed column would have to be regenerated by a pressure swing or another procedure. Instead, continuous membrane processes would be advantageous for the envisioned CO_2/CH_4 separation. Hence, we fabricated CB6-, MIL-101-, and CB6@MIL-101-36-based mixed matrix membranes (MMMs) to demonstrate the superiority of the composite MMM in CO_2/CH_4 separation.

The CH_4 sorption and CO_2/CH_4 selectivity investigation of CB6, MIL-101, and CB6@MIL-101-W (W = 19, 29, 36; Figure S25 and Table S2) indicated a slightly enhanced CH_4 sorption for the composite compared with CB6 and MIL-101. This can be traced back to the enhanced composite affinity towards CH_4 based on the Q_{st}^0 values of 18.1, 19.6, 24.2, 25.6, and 26.3 kJ mol^{-1} for MIL-101, CB6, and CB6@MIL-101-W (W = 19, 29, 36), respectively (Figure S25b). Nevertheless, the composites still exhibited an increased CO_2/CH_4 selectivity for a CO_2/CH_4 mixture (2:98) at 1.0 bar over the individual components. The IAST selectivities for CB6, MIL-101, and CB6@MIL-101-W (W = 19, 29, 36) were found to be 12.7, 17, 20, 27, and 29 at 293 K and 1.0 bar (Figure S25d). To further confirm this superiority of the CB6@MIL-101 composites, we fabricated MMMs[15] of 16 wt% CB6, MIL-101, and CB6@MIL-101-36 in Matrimid as the polymer matrix (Figure S34). The membranes were tested for their mixed-gas separation properties in a binary mixture of CO_2/CH_4 (50:50 v/v) at 25 °C and 3 bar transmembrane pressure. Additionally, all MMMs were characterized by SEM imaging and SEM-EDX mapping to confirm the homogeneous distribution of the filler particles in the polymer matrix (Figures S35 and S36).

The MMMs of CB6/Matrimid simultaneously displayed slightly reduced permeability but also slightly increased selectivity for CO_2/CH_4 compared to the neat polymer membrane (Figure S40 and Table S5). The reduction in permeability can be attributed to the almost non-existent pore volume of CB6. Hence, CB6 alone can be considered a nonporous filler with high CO_2 affinity, which leads to the increased selectivity.[31] MIL-101/Matrimid MMMs showed the expected enhanced CO_2 (from 7 Barrer to 16 Barrer) and CH_4 (from 0.2 Barrer to 0.4 Barrer) permeability but no increase in selectivity. The distinct enhancement in permeability can be assigned to the high pore volume of MIL-101. However, the large pores of MIL-101 and mediocre affinity to

CO_2 over CH_4 prevent a favorable adsorption of CO_2 and thus an increase in selectivity. For CB6@MIL-101-36/Matrimid MMMs, an enhancement of the CO_2 permeability to 15 Barrer up from 7 Barrer for the neat polymer membrane was observed. Moreover, the CO_2/CH_4 selectivity improved from 39 to 46. The encapsulation of CB6 in MIL-101 can therefore, as predicted in the IAST model, increase the affinity for CO_2 and lead to a higher selectivity while only slightly reducing the permeability due to the smaller pore volume compared to pure MIL-101 as a filler. Thus, by encapsulating porous CB6 cages in MIL-101, the CO_2 uptake and the CO_2/N_2 and CO_2/CH_4 selectivities of the hybrids can be enhanced.

α-Cyclodextrin (α-CD) was used as another porous organic cage for its comparatively smaller outer diameter (ca. 1.4 nm), which is smaller than the larger window (1.5 nm) of MIL-101, and for its various properties including CO_2 capture to form host/guest inclusion complexes.[32] α-CD was quantitatively merged into the composite by the incipient-wetness impregnation method thanks to its very good water solubility (see the Supporting Information for details). However, it should be noted that compared with cucurbit-[6]uril, α-CD has a much lower affinity towards CO_2. This is the reason why a significant CO_2 uptake or separation enhancement was not observed under the current experimental conditions (Tables S6 and S7). Still, these results with α-CD indicate the importance of choosing the right porous organic cage in preparing a targeted POC@MOF composite for a specific application.

Conclusion

In summary, we have confined a porous organic cage into the nanocages of MIL-101 by the incipient-wetness impregnation method, obtaining the host-in-host adsorbent CB6@MIL-101, which showed enhanced performance in selective CO_2 adsorption and separation at low pressures. We believe that the host-in-host concept can be extended to encapsulate a broad range of POCs into porous crystalline materials such as MOFs, either by in situ assembly of host MOFs or by post-impregnation methods. This can lead to advanced porous materials, which could combine the merits (such as tailor-made intrinsic pores for molecule capture and separation,[9b,c] enzymatic catalysis,[33] confinement effects[34]) of porous organic molecules and the tunable, highly ordered architectures of functional MOFs.[3]

Acknowledgements

J.L. acknowledges support from the Hoffmann Institute of Advanced Materials (HIAM), Shenzhen Polytechnic.

Conflict of interest

The authors declare no conflict of interest.

Keywords: carbon dioxide uptake · cucurbituril · hybrid materials · metal–organic frameworks · porous organic cages

How to cite: *Angew. Chem. Int. Ed.* **2020**, *59*, 6068–6073
Angew. Chem. **2020**, *132*, 6124–6129

[1] a) A. G. Slater, A. I. Cooper, *Science* **2015**, *348*, aaa8075; b) J. Wang, L. Huang, R. Yang, Z. Zhang, J. Wu, Y. Gao, Q. Wang, D. O'Hare, Z. Zhong, *Energy Environ. Sci.* **2014**, *7*, 3478–3518; c) R. S. Haszeldine, *Science* **2009**, *325*, 1647–1652.
[2] J. Li, A. Corma, J. Yu, *Chem. Soc. Rev.* **2015**, *44*, 7112–7127.
[3] a) H. Furukawa, K. E. Cordova, M. O'Keeffe, O. M. Yaghi, *Science* **2013**, *341*, 1230444; b) Z. Zhang, Z.-Z. Yao, S. Xiang, B. Chen, *Energy Environ. Sci.* **2014**, *7*, 2868–2899; c) K. Sumida, D. L. Rogow, J. A. Mason, T. M. McDonald, E. D. Bloch, Z. R. Herm, T. H. Bae, J. R. Long, *Chem. Rev.* **2012**, *112*, 724–781; d) J. Liu, P. K. Thallapally, B. P. McGrail, D. R. Brown, J. Liu, *Chem. Soc. Rev.* **2012**, *41*, 2308–2322; e) J.-R. Li, Y. Ma, M. C. McCarthy, J. Sculley, J. Yu, H.-K. Jeong, P. B. Balbuena, H.-C. Zhou, *Coord. Chem. Rev.* **2011**, *255*, 1791–1823; f) Y.-S. Bae, R. Q. Snurr, *Angew. Chem. Int. Ed.* **2011**, *50*, 11586–11596; *Angew. Chem.* **2011**, *123*, 11790–11801.
[4] a) K. Adil, Y. Belmabkhout, R. S. Pillai, A. Cadiau, P. M. Bhatt, A. H. Assen, G. Maurin, M. Eddaoudi, *Chem. Soc. Rev.* **2017**, *46*, 3402–3430; b) Y.-B. Huang, J. Liang, X.-S. Wang, R. Cao, *Chem. Soc. Rev.* **2017**, *46*, 126–157; c) C. Janiak, J. K. Vieth, *New J. Chem.* **2010**, *34*, 2366–2388.
[5] a) C. S. Diercks, O. M. Yaghi, *Science* **2017**, *355*, eaal1585; b) S. Kandambeth, K. Dey, R. Banerjee, *J. Am. Chem. Soc.* **2019**, *141*, 1807–1822.
[6] a) G. Zhang, M. Mastalerz, *Chem. Soc. Rev.* **2014**, *43*, 1934–1947; b) M. Mastalerz, *Acc. Chem. Res.* **2018**, *51*, 2411–2422.
[7] a) J. Murray, K. Kim, T. Ogoshi, W. Yao, B. C. Gibb, *Chem. Soc. Rev.* **2017**, *46*, 2479–2496; b) Z. Liu, S. K. M. Nalluri, J. F. Stoddart, *Chem. Soc. Rev.* **2017**, *46*, 2459–2478.
[8] a) G. Zhang, O. Presly, F. White, I. M. Oppel, M. Mastalerz, *Angew. Chem. Int. Ed.* **2014**, *53*, 1516–1520; *Angew. Chem.* **2014**, *126*, 1542–1546; b) M. Mastalerz, M. W. Schneider, I. M. Oppel, O. Presly, *Angew. Chem. Int. Ed.* **2011**, *50*, 1046–1051; *Angew. Chem.* **2011**, *123*, 1078–1083; c) J. Tian, P. K. Thallapally, S. J. Dalgarno, P. B. McGrail, J. L. Atwood, *Angew. Chem. Int. Ed.* **2009**, *48*, 5492–5495; *Angew. Chem.* **2009**, *121*, 5600–5603; d) T. Tozawa, J. T. A. Jones, S. I. Swamy, S. Jiang, D. J. Adams, S. Shakespeare, R. Clowes, D. Bradsaw, T. Hasell, S. Y. Chong, C. Tang, S. Thompson, J. Parker, A. Trewin, J. Bacsa, A. M. Z. Slawin, A. Steiner, A. I. Cooper, *Nat. Mater.* **2009**, *8*, 973–978.
[9] a) A. Chaix, G. Mouchaham, A. Shkurenko, P. Hoang, B. Moosa, P. M. Bhatt, K. Adil, K. N. Salama, M. Eddaoudi, N. M. Khashab, *J. Am. Chem. Soc.* **2018**, *140*, 14571–14575; b) K. J. Hartlieb, J. M. Holcroft, P. Z. Moghadam, N. A. Vermeulen, M. M. Algaradah, M. S. Nassar, Y. Y. Botros, R. Q. Snurr, J. F. Stoddart, *J. Am. Chem. Soc.* **2016**, *138*, 2292–2301; c) R. A. Smaldone, R. S. Forgan, H. Furukawa, J. J. Gassensmith, A. M. Slawin, O. M. Yaghi, J. F. Stoddart, *Angew. Chem. Int. Ed.* **2010**, *49*, 8630–8634; *Angew. Chem.* **2010**, *122*, 8812–8816; d) R. S. Patil, D. Banerjee, C. Zhang, P. K. Thallapally, J. L. Atwood, *Angew. Chem. Int. Ed.* **2016**, *55*, 4523–4526; *Angew. Chem.* **2016**, *128*, 4599–4602; e) S. Lim, H. Kim, N. Selvapalam, K.-J. Kim, S. J. Cho, G. Seo, K. Kim, *Angew. Chem.* **2008**, *120*, 3400–3403; f) E. Li, Y. Zhou, R. Zhao, K. Jie, F. Huang, *Angew. Chem. Int. Ed.* **2019**, *58*, 3981–3985; *Angew. Chem.* **2019**, *131*, 4021–4025.

[10] a) S. J. Barrow, S. Kasera, M. J. Rowland, J. del Barrio, O. A. Scherman, *Chem. Rev.* **2015**, *115*, 12320 – 12406; b) K. I. Assaf, W. M. Nau, *Chem. Soc. Rev.* **2015**, *44*, 394 – 418; c) L. Isaacs, *Chem. Commun.* **2009**, 619 – 629; d) K. Kim, J. Murray, N. Selvapalam, Y. H. Ko, I. Hwang, *Cucurbiturils: Chemistry, Supramolecular Chemistry and Applications.* World Scientific Publishing Company, Singapore, **2018**.

[11] a) K. Kim, N. Selvapalam, Y. H. Ko, K. M. Park, D. Kim, J. Kim, *Chem. Soc. Rev.* **2007**, *36*, 267 – 279; b) D. Bardelang, K. A. Udachin, D. M. Leek, J. C. Margeson, G. Chan, C. I. Ratcliffe, J. A. Ripmeester, *Cryst. Growth Des.* **2011**, *11*, 5598 – 5614; c) H. Kim, Y. Kim, M. Yoon, S. Lim, S. M. Park, G. Seo, K. Kim, *J. Am. Chem. Soc.* **2010**, *132*, 12200 – 12202; d) X.-L. Ni, X. Xiao, H. Cong, L.-L. Liang, K. Cheng, X.-J. Cheng, N.-N. Ji, Q.-J. Zhu, S.-F. Xue, Z. Tao, *Chem. Soc. Rev.* **2013**, *42*, 9480 – 9508.

[12] T. Hasell, A. I. Cooper, *Nat. Rev. Mater.* **2016**, *1*, 16053.

[13] a) T. Hasell, S. Y. Chong, K. E. Jelfs, D. J. Adams, A. I. Cooper, *J. Am. Chem. Soc.* **2012**, *134*, 588 – 598; b) S. Du, C. Hu, J.-C. Xiao, H. Tan, W. Liao, *Chem. Commun.* **2012**, *48*, 9177 – 9179; c) Q. Li, W. Zhang, O. S. Miljanic, C. H. Sue, Y. L. Zhao, L. Liu, C. B. Knobler, J. F. Stoddart, O. M. Yaghi, *Science* **2009**, *325*, 855 – 859; d) C. Valente, E. Choi, M. E. Belowich, C. J. Doonan, Q. Li, T. B. Gasa, Y. Y. Botros, O. M. Yaghi, J. F. Stoddart, *Chem. Commun.* **2010**, *46*, 4911 – 4913.

[14] a) O. Buyukcakir, Y. Seo, A. Coskun, *Chem. Mater.* **2015**, *27*, 4149 – 4155; b) Y. Zhang, J. Duan, D. Ma, P. Li, S. Li, H. Li, J. Zhou, X. Ma, X. Feng, B. Wang, *Angew. Chem. Int. Ed.* **2017**, *56*, 16313 – 16317; *Angew. Chem.* **2017**, *129*, 16531 – 16535; c) M. J. Klemes, Y. Ling, C. Ching, C. Wu, L. Xiao, D. E. Helbling, W. R. Dichtel, *Angew. Chem. Int. Ed.* **2019**, *58*, 12049 – 12053; *Angew. Chem.* **2019**, *131*, 12177 – 12181; d) S. Y. Jon, N. Selvapalam, D. H. Oh, J.-K. Kang, S.-Y. Kim, Y. J. Jeon, J. W. Lee, K. Kim, *J. Am. Chem. Soc.* **2003**, *125*, 10186 – 10187; e) Y. Ahn, Y. Jang, N. Selvapalam, G. Yun, K. Kim, *Angew. Chem. Int. Ed.* **2013**, *52*, 3140 – 3144; *Angew. Chem.* **2013**, *125*, 3222 – 3226.

[15] a) J. Dechnik, J. Gascon, C. J. Doonan, C. Janiak, C. J. Sumby, *Angew. Chem. Int. Ed.* **2017**, *56*, 9292 – 9310; *Angew. Chem.* **2017**, *129*, 9420 – 9439; b) Y. Cheng, Z. Wang, D. Zhao, *Ind. Eng. Chem. Res.* **2018**, *57*, 4139 – 4169; c) A. F. Bushell, P. M. Budd, M. P. Attfield, J. T. Jones, T. Hasell, A. I. Cooper, P. Bernardo, F. Bazzarelli, G. Clarizia, J. C. Jansen, *Angew. Chem. Int. Ed.* **2013**, *52*, 1253 – 1256; *Angew. Chem.* **2013**, *125*, 1291 – 1294; d) G. Zhu, F. Zhang, M. P. Rivera, X. Hu, G. Zhang, C. W. Jones, R. P. Lively, *Angew. Chem. Int. Ed.* **2019**, *58*, 2638 – 2643; *Angew. Chem.* **2019**, *131*, 2664 – 2669.

[16] a) A. I. Cooper, *Angew. Chem. Int. Ed.* **2011**, *50*, 996 – 998; *Angew. Chem.* **2011**, *123*, 1028 – 1030; b) A. Avellaneda, P. Valente, A. Burgun, J. D. Evans, A. W. Markwell-Heys, D. Rankine, D. J. Nielsen, M. R. Hill, C. J. Sumby, C. J. Doonan, *Angew. Chem. Int. Ed.* **2013**, *52*, 3746 – 3749; *Angew. Chem.* **2013**, *125*, 3834 – 3837.

[17] G. Férey, C. Mellot-Draznieks, C. Serre, F. Millange, J. Dutour, S. Surblé, I. Margiolaki, *Science* **2005**, *309*, 2040 – 2042.

[18] T. Bogaerts, A. Van Yperen-De Deyne, Y.-Y. Liu, F. Lynen, V. Van Speybroeck, P. Van Der Voort, *Chem. Commun.* **2013**, *49*, 8021 – 8023.

[19] X. Qiu, W. Zhong, C. Bai, Y. Li, *J. Am. Chem. Soc.* **2016**, *138*, 1138 – 1141.

[20] Q. Yang, Q. Xu, H.-L. Jiang, *Chem. Soc. Rev.* **2017**, *46*, 4774 – 4808.

[21] a) Y. Ban, Z. Li, Y. Li, Y. Peng, H. Jin, W. Jiao, A. Guo, P. Wang, Q. Yang, C. Zhong, W. Yang, *Angew. Chem. Int. Ed.* **2015**, *54*, 15483 – 15487; *Angew. Chem.* **2015**, *127*, 15703 – 15707; b) I. Cota, F. Fernandez Martinez, *Coord. Chem. Rev.* **2017**, *351*, 189 – 204.

[22] a) K. A. Kovalenko, V. P. Fedin, *Russ. Chem. Bull.* **2016**, *65*, 1406 – 1417; b) F. P. Kinik, A. Uzun, S. Keskin, *ChemSusChem* **2017**, *10*, 2842 – 2863.

[23] H. S. El-Sheshtawy, B. S. Bassil, K. I. Assaf, U. Kortz, W. M. Nau, *J. Am. Chem. Soc.* **2012**, *134*, 19935 – 19941.

[24] a) P. Horcajada, C. Serre, M. Vallet-Regi, M. Sebban, F. Taulelle, G. Ferey, *Angew. Chem. Int. Ed.* **2006**, *45*, 5974 – 5978; *Angew. Chem.* **2006**, *118*, 6120 – 6124; b) Q. Yan, Y. Lin, C. Kong, L. Chen, *Chem. Commun.* **2013**, *49*, 6873 – 6875.

[25] D. Bardelang, A. Brinkmann, C. I. Ratcliffe, J. A. Ripmeester, V. V. Terskikh, K. A. Udachin, *CrystEngComm* **2014**, *16*, 3788.

[26] A. Day, A. P. Arnold, R. J. Blanch, B. Snushall, *J. Org. Chem.* **2001**, *66*, 8094 – 8100.

[27] M. Thommes, K. Kaneko, A. V. Neimark, J. P. Olivier, F. Rodriguez-Reinoso, J. Rouquerol, K. S. W. Sing, *Pure Appl. Chem.* **2015**, *87*, 1051 – 1069.

[28] P. L. Llewellyn, S. Bourrelly, C. Serre, A. Vimont, M. Daturi, L. Hamon, G. D. Weireld, J.-S. Chang, D.-Y. Hong, Y. K. Hwang, S. H. Jhung, G. Férey, *Langmuir* **2008**, *24*, 7245 – 7250.

[29] A. J. Emerson, A. Chahine, S. R. Batten, D. R. Turner, *Coord. Chem. Rev.* **2018**, *365*, 1 – 22.

[30] a) J. Tian, J. Liu, J. Liu, P. K. Thallapally, *CrystEngComm* **2013**, *15*, 1528 – 1531; b) N. A. A. Qasem, N. U. Qadir, R. Ben-Mansour, S. A. M. Said, *J. CO2 Util.* **2017**, *22*, 238 – 249.

[31] A. Nuhnen, D. Dietrich, S. Millan, C. Janiak, *ACS Appl. Mater. Interfaces* **2018**, *10*, 33589 – 33600.

[32] a) G. Crini, *Chem. Rev.* **2014**, *114*, 10940 – 10975; b) T.-L. Neoh, H. Yoshii, T. Furuta, *J. Inclusion Phenom. Macrocyclic Chem.* **2006**, *56*, 125 – 133; c) J. Szejtli, *Chem. Rev.* **1998**, *98*, 1743 – 1753.

[33] a) R. Villalonga, R. Cao, A. Fragoso, *Chem. Rev.* **2007**, *107*, 3088 – 3116; b) Y. Murakami, J. Kikuchi, Y. Hisaeda, O. Hayashida, *Chem. Rev.* **1996**, *96*, 721 – 758; c) W. L. Mock, T. A. Irra, J. P. Wepsiec, T. L. Manimaran, *J. Org. Chem.* **1983**, *48*, 3619 – 3620; d) C. Goehry, M. Besora, F. Maseras, *ACS Catal.* **2015**, *5*, 2445 – 2451.

[34] a) Y. Chen, B. Yu, Y. Cui, S. Xu, J. Gong, *Chem. Mater.* **2019**, *31*, 1289 – 1295; b) Z. Y. Zhang, Y. Chen, Y. Liu, *Angew. Chem. Int. Ed.* **2019**, *58*, 6028 – 6032; *Angew. Chem.* **2019**, *131*, 6089 – 6093.

Manuscript received: December 13, 2019
Accepted manuscript online: January 8, 2020
Version of record online: February 3, 2020

